

Cite this: *Mater. Adv.*, 2024,  
5, 3499

# Optimization of extraction conditions to synthesize green carbon nanodots using the Maillard reaction

Duyen H.H. Nguyen,<sup>id</sup> \*<sup>abc</sup> Arjun Muthu,<sup>id</sup> <sup>cd</sup> Hassan El-Ramady,<sup>ae</sup> Lajos Daróczy,<sup>f</sup> Lajos Nagy,<sup>g</sup> Sándor Kéki,<sup>id</sup> <sup>g</sup> Áron Béni,<sup>d</sup> Istvan Csarnovics<sup>id</sup> <sup>h</sup> and József Prokisch<sup>a</sup>

Carbon nanodots (CNDs) are a class of nanoparticles with unique optical properties with broad applications in various fields. However, synthesizing CNDs with high fluorescence intensity and small size using a green solvent and low temperature remains challenging. In this study, we investigated the use of the Maillard reaction for synthesizing CNDs and optimized the reaction conditions at 120 °C for 12 h to achieve CNDs with desirable properties. The results showed that glycine was the most effective amino acid for CNDs formation when combined with sucrose. A molar ratio of 1:1 for glycine:sucrose resulted in the highest fluorescence intensity. The fluorescence intensity increased remarkably with 40% ethanol as the extraction solvent. However, a high ethanol concentration (above 60%) had an inverse relationship with CNDs' fluorescence intensity, indicating that a high concentration of ethanol solution prevented the Schiff base formation. The purified CNDs (M-CNDs) were characterized using fluorescence spectrophotometry, UV-Vis spectroscopy, Raman spectroscopy, and TEM techniques. These findings provide a purification process of sustainable CNDs using the Maillard reaction and green solvents with optimized conditions and low temperatures.

Received 12th January 2024,  
Accepted 28th February 2024

DOI: 10.1039/d4ma00037d

rsc.li/materials-advances

## Introduction

Carbon nanodots (CNDs) with sizes smaller than 10 nm have been reported for the first time since 2004.<sup>1</sup> CNDs are attractive because of their intense fluorescent properties, high water solubility, stability, and ease of functionalization.<sup>1–3</sup> Since their discovery, CNDs have garnered considerable attention across various sectors due to their highly fluorescent properties and

potential applications in diverse fields, including biomedical,<sup>4</sup> food safety,<sup>5</sup> and the bio-electrical industry.<sup>6</sup> In the food industry, CNDs have emerged as promising compounds for developing high-sensitivity probes to detect contaminants such as heavy metals,<sup>7,8</sup> pesticides,<sup>9,10</sup> and food additives,<sup>11,12</sup> as well as packaging materials to detect spoilage of foods,<sup>13–15</sup> and even detecting foodborne pathogens.<sup>16,17</sup>

Notably, CNDs are low-toxicity compounds<sup>18</sup> and have been used in biocompatible drug delivery and bioimaging applications.<sup>19,20</sup> Studies show that nitrogen-doped CNDs with surface modifications do not harm human lung epithelial tissue *in vitro* and can exhibit antioxidant and anti-cancer properties.<sup>21,22</sup> However, there is a research gap to prove that CNDs can be used without any health concerns. CNDs have low cytotoxicity depending on the dose, synthesis process, and precursors.<sup>23–25</sup> Therefore, choosing safe precursors for the synthesis of CNDs is emerging as a promising strategy to enhance their safety for food industry applications.

The Maillard reaction, a complex series of reactions between reducing sugars and amino groups, is a crucial process in the food industry, affecting food's aesthetic, functional, and nutritional properties.<sup>26</sup> This reaction shows a close relationship with the formation of CNDs.<sup>27,28</sup> CNDs are a marker to control the Maillard reaction,<sup>28</sup> directly related to the formation of melanoidins, brown pigments with high aromaticity.<sup>27</sup>

<sup>a</sup> Institute of Animal Science, Faculty of Agricultural and Food Sciences and Environmental Management, Biotechnology and Nature Conservation, University of Debrecen, 138 Böszörményi Street, 4032 Debrecen, Hungary.  
E-mail: nguyen.huu.huong.duyen@agr.unideb.hu

<sup>b</sup> Tay Nguyen Institute for Scientific Research, Vietnam Academy of Science and Technology, 118 Xo Viet Nghe Tinh Street, Da Lat, Vietnam

<sup>c</sup> Doctoral School of Nutrition and Food Science, University of Debrecen, Debrecen, Hungary

<sup>d</sup> Institute of Agricultural Chemistry and Soil Science, Faculty of Agricultural and Food Sciences and Environmental Management, University of Debrecen, 138 Böszörményi Street, 4032 Debrecen, Hungary

<sup>e</sup> Soil and Water Department, Faculty of Agriculture, Kafrelsheikh University, Kafr El-Sheikh 33516, Egypt

<sup>f</sup> Department of Solid State Physics, University of Debrecen, PO Box 400, Debrecen, Hungary

<sup>g</sup> Department of Applied Chemistry, Faculty of Sciences and Technology, University of Debrecen, Egyetem tér 1, H-4032 Debrecen, Hungary

<sup>h</sup> Department of Experimental Physics, University of Debrecen, Debrecen, Hungary



In this study, we investigated the use of amino acids and sucrose as a model system of the Maillard reaction for synthesizing CNDs and optimizing the reaction conditions to achieve CNDs with desirable properties. Using safe precursors (amino acids and sugars) from a fundamental food reaction is advantageous for the safety of CNDs. Furthermore, using lower temperatures and greener solvents, we aim to reduce the formation of toxins in the synthesis process and create safer CNDs with standardized quality. Purified CNDs were characterized using transmission electron microscopy (TEM), fluorescence, Raman, and UV-Vis spectroscopy techniques. The obtained CNDs were used as a standard to measure the concentration of CNDs forming in the breadmaking process.

## Materials and methods

### Materials

Amino acids (L-arginine, glycine, L-tyrosine, L-proline, L-glutamine, and L-phenylalanine) and sucrose were obtained from Vital-Trend Ltd (Budapest, Hungary). Hydrochloric acid ( $1.0 \text{ mol L}^{-1}$ ), ethanol ( $\geq 99.5\%$ ), and sodium hydroxide solution ( $0.01 \text{ mol L}^{-1}$ ) were used as-obtained (VWR International Ltd, Pennsylvania, United States). Ultrapure water was used in all the experiments. Fresh bread was bought from the ALDI supermarket on the experiment day.

### Characterization

The morphology and particle size of CNDs were measured using a transmission electron microscope (TEM) of JEM-2000FXII (JEOL Ltd, Tokyo, Japan). A Lambda 35 UV-Vis spectrophotometer (Norwalk, USA) was used to measure the ultraviolet-visible (UV-vis) spectra in the 200–600 nm range. Olympus Endosonic Ultrasonicator (Olympus Co., Tokyo, Japan) was used for ultrasound steps. Raman spectra were measured using a LabRAM HR Evolution Confocal Raman Microscope (Horiba, Ltd, Kyoto, Japan).<sup>29</sup> The fluorescence spectra were measured using a Spectrofluorometer FP-8500, Jasco, Oklahoma, United States.<sup>30</sup>

### Experimental design

The synthesis method of CNDs from the Maillard reaction was based on the published procedure with modification.<sup>25</sup> The optimal conditions for the Maillard reaction were investigated to achieve CNDs with high fluorescence intensity and small size following three experiments, which are illustrated in Fig. 1. (1) Initially, six amino acids—L-arginine (Arg), glycine (Gly), L-tyrosine (Tyr), L-proline (Pro), L-glutamine (Gln), and L-phenylalanine (Phe) were selected as precursors in combination with sucrose to form CNDs. (2) Following the selection of an amino acid that formed the highest quality CNDs, the ratio between amino acid and sucrose was examined using nine combinations, including 2 mmol: 0 mmol, 1.75 mmol: 0.25 mmol, 1.5 mmol: 0.5 mmol, 1.25 mmol: 0.75 mmol, 1 mmol: 1 mmol, 0.75 mmol: 1.25 mmol, 0.5 mmol: 1.5 mmol, 0.25 mmol: 1.75 mmol, and 0 mmol: 2 mmol. (3) Subsequently, various extraction solvents were assessed using nine different options: control (DI water), DI water

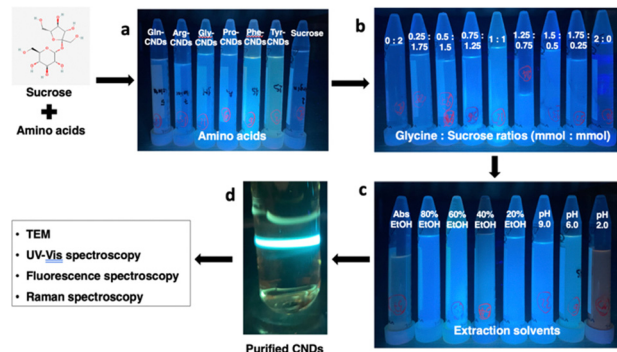


Fig. 1 Schematic of the experimental design listing three experiments and obtaining purified carbon nanodots (CNDs) with authentic images taken under a UV lamp. (a) The effect of different amino acids on the fluorescence of amino acid-based carbon nanodots (AA-CNDs) including L-arginine (Arg), glycine (Gly), L-tyrosine (Tyr), L-proline (Pro), L-glutamine (Gln), and L-phenylalanine (Phe); (b) the impact of the ratio between glycine and sucrose ( $\text{mmol mmol}^{-1}$ ) on the fluorescence of CNDs (2 mmol: 0 mmol, 1.75 mmol: 0.25 mmol, 1.5 mmol: 0.5 mmol, 1.25 mmol: 0.75 mmol, 1 mmol: 1 mmol, 0.75 mmol: 1.25 mmol, 0.5 mmol: 1.5 mmol, 0.25 mmol: 1.75 mmol, and 0 mmol: 2 mmol); (c) the effect of the extraction solvents on the fluorescence of CNDs, including Control (DI water), DI water adjusted to pH 2.0, DI water adjusted to pH 9.0, ethanol (EtOH) at 20%, EtOH 40%, EtOH 60%, EtOH 80%, and absolute EtOH; (d) the purified CNDs characterized with TEM, UV-Vis, fluorescence, and Raman spectroscopy.

adjusted to pH 2.0, DI water adjusted to pH 9.0, ethanol (EtOH) at 20%, EtOH 40%, EtOH 60%, EtOH 80%, and absolute EtOH. The optimal conditions were determined based on fluorescent spectra, and each treatment was performed in triplicate.

To synthesize and purify CNDs, the solution was heated at  $120 \text{ }^\circ\text{C}$  for 12 h and naturally cooled to room temperature. Cold ethanol was added to the product at a 1 : 1 (v/v) ratio to remove residual amino acids and incubated for 30 minutes at  $-20 \text{ }^\circ\text{C}$ . Subsequently, the mixture was centrifuged at 10 000 rpm for 30 min. The supernatant obtained was passed through a cellulose column, and the resulting solution was collected and filtered through a  $0.22 \text{ }\mu\text{m}$  filter. After freeze-drying, the powder of the Maillard reaction-derived carbon nanodots (MR-CNDs) was collected and stored for future use. The purified CNDs were characterized using TEM, and Raman, UV-Vis, and fluorescence spectroscopy techniques.

### Statistical analysis

The statistical results were analyzed using IBM SPSS version 25.0 (New York, USA). TEM images and particle distribution were processed using ImageJ software version 1.54D, developed by the National Institutes of Health (New York, USA). All charts were illustrated using GraphPad Prism version 9.0 (California, USA).

## Results and discussion

### Optimization for the synthesis of carbon nanodots using the Maillard reaction

To investigate the impact of the extraction conditions on the formation of carbon nanodots (CNDs) through the Maillard reaction, all parameters, except for the studied variable, were



kept constant according to the following procedure. Initially, glycine (0.053 g, 1 mmol) and sucrose (0.180 g, 1 mmol) were dissolved in 20 mL of deionized (DI) water. The solution underwent heating at 120 °C for 12 h, followed by natural cooling to room temperature. Subsequently, it was mixed with cold ethanol in a 1 : 1 ratio (v/v), and the mixture was incubated in the freezer for 30 min. Afterward, centrifugation at 10 000 rpm for 30 min separated the supernatant, which was then passed through a cellulose column to eliminate impurities. The resulting liquid was filtered through a 0.22 μm filter and subjected to freeze-drying. The obtained powder represented the Maillard reaction-derived carbon nanodots (MR-CNDs) product. This method was modified at a lower temperature<sup>31</sup> to prevent the formation of toxic compounds such as 5-HMF during the Maillard reactions.<sup>32</sup>

The fluorescence signal was measured using a fluorescence spectrophotometer with an excitation wavelength selected after scanning the excitation and emission wavelengths of standardized CNDs, as discussed in the subsequent section.

### The effect of different amino acids on the formation of CNDs

The Maillard reaction is a complex series of reactions between reducing sugars and amino acids.<sup>26</sup> These reactions can lead to the formation of various new compounds, including CNDs. Furthermore, CNDs have been reported as a marker to control the Maillard reaction.<sup>28</sup> In this study, the relationship between the Maillard reaction and the formation of CNDs was understood through a chosen study model between amino acids and sucrose. Fig. 2 illustrates the distinct fluorescent spectra of CNDs generated from sucrose and various amino acids, including tyrosine, proline, glycine, arginine, glutamine, and phenylalanine. The distinct excitation wavelengths for each amino acid are highlighted in the figure: 340 nm for tyrosine, 360 nm for proline, and 380 nm for glycine, arginine, glutamine, and phenylalanine. The fluorescence intensity of the different amino acids considerably varies (Fig. 2). Glycine-based carbon nanodots have the highest fluorescence intensity, followed by phenylalanine, proline, glutamate, arginine, and tyrosine, as shown in Fig. 2. It is likely due to glycine's enhanced reactivity

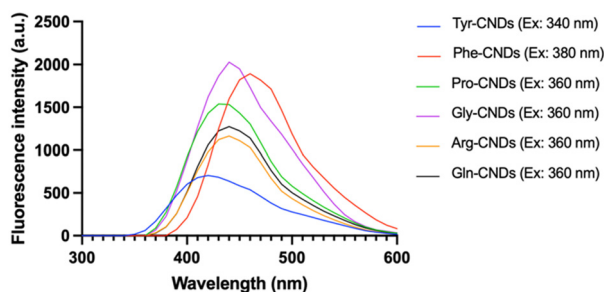


Fig. 2 Fluorescent emission spectra of carbon nanodots (CNDs) formed from various amino acids and sucrose. The emission spectra plotted with fluorescence intensity (a.u.) with the excitation wavelength depending on the type of amino acid: 340 nm for tyrosine (Tyr), 360 nm for proline (Pro), glycine (Gly), arginine (Arg), glutamine (Gln), and 380 nm for phenylalanine (Phe).

in the Maillard reaction, which is attributed to its higher susceptibility for forming Schiff bases, intermediate products of the Maillard reaction. These Schiff bases can then react to form other fluorescent compounds, such as melanoidins and brown pigments. These melanoidins are essential precursors for forming CNDs.<sup>27</sup>

The different chemical structures of the amino acids can explain this phenomenon. Tyrosine and phenylalanine contain aromatic rings known for fluorescence.<sup>33</sup> Proline has a ring structure, but it is not aromatic. Glycine and arginine are both non-aromatic amino acids. Glutamine is an amino acid that can be converted to glutamine, a non-fluorescent amino acid.<sup>34</sup> Fluorescence intensity depends on the structure of amino acids; the simpler the structure, the higher the formation of CNDs, and the higher the fluorescence intensity, as depicted in Fig. 3. Fig. 3 illustrates the fluorescence intensity of amino acids (without the synthesis process) and amino acid-based CNDs. Although phenylalanine resulted in the highest intensity ( $724.0 \pm 4.0$ ), the intensity of Phe-CNDs ( $1900.0 \pm 9.1$ ) was lower than that of Gly-CNDs ( $2024.0 \pm 3.7$ ), where glycine was the weakest in the fluorescence intensity at the beginning ( $134.9 \pm 1.9$ ). These findings suggest that glycine is a good precursor for synthesizing CNDs with high fluorescence intensity.

### Effect of the ratio between glycine and sugars ( $\text{mmol mmol}^{-1}$ ) on the formation of CNDs

Based on glycine's selection as the precursor in the previous experiment, the excitation wavelength of 360 nm was readily adopted to synthesize CNDs. Fig. 4 shows the fluorescence emission spectra of CNDs formed from different ratios between glycine and sucrose ( $\text{mmol mmol}^{-1}$ ). The fluorescence intensity of the CNDs increased with increasing glycine content until the ratio of 1 mmol glycine to 1 mmol sucrose (Fig. 4). This is likely because glycine is more susceptible to forming Schiff bases. However, when the amount of glycine in the mixture continuously increased, the fluorescence intensity was remarkably

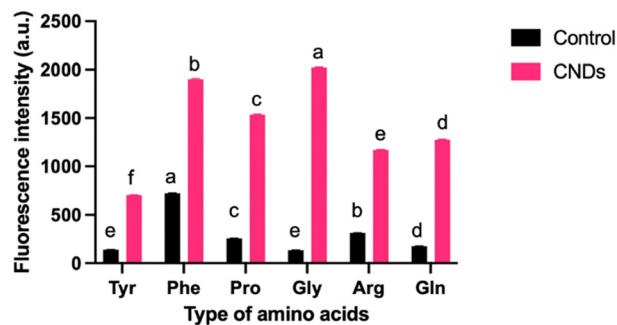


Fig. 3 Fluorescence intensity (a.u.) of amino acid-based carbon nanodots (CNDs) and amino acids (Control). Each amino acid (AA) – tyrosine (Tyr), proline (Pro), glycine (Gly), arginine (Arg), glutamine (Gln), and phenylalanine (Phe) – was excited at specific wavelengths (340 nm for Tyr, 360 nm for Pro, Gly, Arg, Gln, and 380 nm for Phe). The error bars indicate the standard deviations of the triplicate sample. Different letters (a–f) present a significant difference with a confidence interval of 95% compared with other samples at the same treatment.



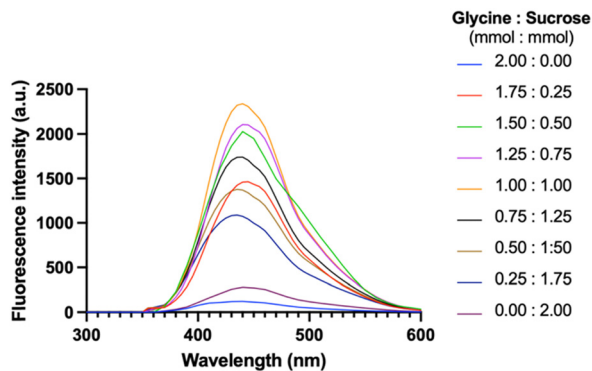


Fig. 4 Fluorescent emission spectra of CNDs formed at different ratios of glycine and sucrose (mmol/mmol), measured with the excitation wavelength at 360 nm. Nine ratios were studied in this experiment, including 2 mmol: 0 mmol, 1.75 mmol: 0.25 mmol, 1.5 mmol: 1.25 mmol, 0.75 mmol: 1 mmol, 1 mmol: 0.75 mmol, 1.25 mmol: 0.5 mmol, 0.5 mmol: 1.5 mmol, 0.25 mmol: 1.75 mmol, and 0 mmol: 2 mmol.

reduced. This trend was attributed to the excess glycine interfering with the formation of Schiff bases, which are essential for CNDs formation. Overall, it suggests that the fluorescence intensity of CNDs can be controlled by adjusting the glycine:sucrose ratio. The ratio between glycine and sucrose was maintained at 1:1 (mmol mmol<sup>-1</sup>). It exhibited the highest fluorescence intensity. This could be useful for developing CNDs with specific fluorescence properties for different applications.

#### Effect of extraction solvents on the formation of CNDs

Fig. 5 depicts the fluorescence intensity of CNDs formed using various extraction solvents, with the control sample extracted using deionized (DI) water at pH 6.0. Comparing different pH extraction solvents, the higher fluorescence intensity of CNDs was obtained when extracted with DI water at pH 9.0. In contrast, pH 2.0 seems to destroy the presence of CNDs. The structure and fluorescence properties of CNDs could be entirely converted by changing the pH of solvents in the reaction.<sup>35</sup> Notably, the highest fluorescence intensity of CNDs was achieved when extracted with 40% ethanol. These results were similar to the previous report,<sup>36</sup> which mentioned that ethanolic solution can significantly enhance the reaction rate of the Maillard reaction, resulting in the browning at 420 nm.

Furthermore, this phenomenon can be attributed to the favorable conditions for forming Schiff bases, crucial intermediates in the Maillard reaction. The Maillard reaction governs the complex interaction between reducing sugars and amino acids, providing strong evidence for the link between the reaction and CNDs formation. In contrast, an inverse relationship is observed between high ethanol concentration (60% – absolute ethanol) and fluorescence intensity of CNDs, with increasing ethanol concentrations hindering the Schiff base formation. These collective findings suggest a tunable control over the fluorescence intensity of CNDs by manipulating the pH of the extraction solvent and ethanol concentration. Specific observations highlight the maximization of fluorescence

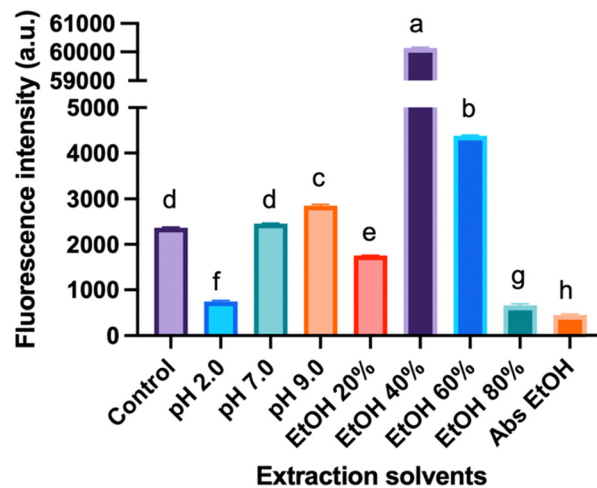


Fig. 5 Formation of CNDs using various extraction solvents: Deionized (DI) water at pH 2.0, pH 7.0, and pH 9.0; different ethanol concentrations (20%, 40%, 60%, 80%, and absolute ethanol). The control sample was extracted with DI water at pH 6.0. Fluorescence intensity measurements were used to assess the formation process. The error bars indicate the standard deviations of the triplicate sample. Different letters (a–h) present a significant difference with a confidence interval of 95%.

intensity at pH 9.0 and the inverse correlation with increasing ethanol concentration, reaching its lowest point with absolute ethanol extraction. These insights are valuable in tailoring CNDs for versatile applications, such as bioimaging or sensing, by optimizing fluorescence properties based on the extraction conditions.

#### Purification and characterization of CNDs prepared using the Maillard reaction

The isolation procedure was performed using 1 mmol of glycine and 1 mmol of sucrose mixed in 20 mL of 40% ethanol solution at 120 °C for 12 h, using a modified published procedure.<sup>25</sup> The resulting solution turned dark brown and exhibited intense fluorescence, from colorless without fluorescence. To extract the M-CNDs further, the mixture was sonicated for 30 min. The obtained solution was then mixed with cold ethanol in a 1:1 ratio (v/v) to remove impurities at –20 °C for 30 min. The mixture was centrifuged at 10 000 rpm for 30 min to obtain the purified M-CNDs. The supernatant was collected and filtered with a 0.22 μm syringe filter. The purified M-CNDs were characterized using TEM, fluorescence, Raman, and UV-Vis spectroscopy (Fig. 6).

TEM images with 10 nm and 1 nm scales revealed the dark spherical morphology of the M-CNDs without any contaminated compounds. The size distribution of the M-CNDs ranged from 1.25 to 4 nm, with an average size of 2.5 ± 0.5 nm based on measurements of almost 300 particles in the TEM image with a scale of 10 nm (Fig. 6A). In Fig. 6E, the UV-vis spectrum of M-CNDs exhibited one peak at 275 nm, indicating the presence of the π–π\* electronic transition in C=C.<sup>37</sup> Blue solid fluorescence of M-CNDs was detected under UV light (Fig. 6B) with a maximum emission wavelength of 438 nm and an



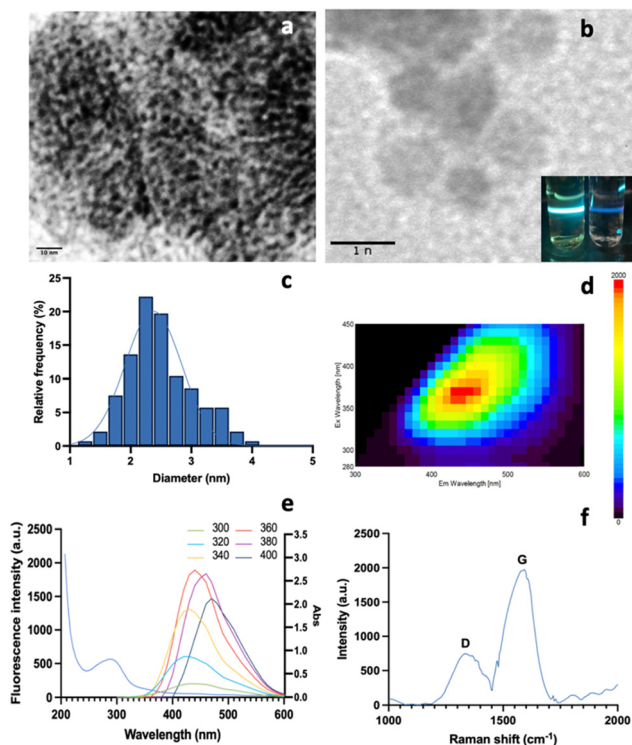


Fig. 6 Characterization of the isolated carbon nanodots prepared using the Maillard reaction (M-CNDs). (a) Transmission Electron Microscopy (TEM) image of M-CNDs with a 10 nm scale. (b) TEM image of M-CNDs with a 1 nm scale with the real image of DI water (left) and M-CNDs solution (right) on the right corner under the UV light. (c) Particle size distribution histogram of M-CNDs with an average diameter of  $2.5 \pm 0.5$  nm. (d) 3-D fluorescence spectra of M-CNDs. (e) 2D emission-excitation-intensity fluorescence spectrum of M-CNDs (right) and UV-Vis spectrum of M-CNDs (left). (f) Raman spectra of M-CNDs.

excitation wavelength of 360 nm (Fig. 6D). These findings were consistent with those from the previous studies that used glucose and lysine or melatonin as starting materials.<sup>25,27</sup>

Furthermore, Raman spectroscopy analysis of the synthesized M-CNDs revealed distinct D and G bands at 1350 and 1580  $\text{cm}^{-1}$ , respectively, as depicted in Fig. 6F. Consistent with established literature, the low-intensity ratio of the D to G band ( $I_D < I_G$ ) underscores the moderate graphitic structure of the M-CNDs, affirming the absence of significant carbonaceous impurities, as corroborated by similar findings in the reference study.<sup>38</sup> Overall, the results explain the successful isolation and characterization of M-CNDs with nanosized, intense fluorescence properties, which could be used as a safe carbon nanodot source for various applications.

#### Use of M-CNDs as a standard for detecting CNDs in food samples using a fluorescent spectrophotometer

To evaluate the purity of M-CNDs and quantitatively determine the carbon content of M-CNDs stock solution, the purified M-CNDs were analyzed using an elemental analyzer, resulting in a total carbon content in the stock M-CNDs solution of 0.326%. Based on the carbon content, the concentration of the stock standard was  $3260 \text{ mg dm}^{-3}$ . Standard curves were

generated by measuring the intensity of the fluorescent spectrum at the excitation wavelength of 360 nm across a range of M-CNDs concentrations. The standard curve was prepared freshly on the measurement day. The resulting calibration curve for CNDs had a linear relationship for a five-point calibration curve in the concentration range from 0 to  $3200 \text{ mg dm}^{-3}$  (Fig. 7). The reproducibility of measurement was below 0.1%. The calculated detection limit of the method was  $0.14 \text{ mg dm}^{-3}$ .

Inter-day variation was also assessed, and a measurement was carried out with a standard addition method. The inter-day variation of the method was less than 0.1%. The calibration and the standard addition methods gave the same concentration result values.

Along with the obtained standard curve in Fig. 7, the concentration of CNDs in breadmaking, including dough, bread crust, and bread crumb, was measured. Note that 1 g of the sample was mixed with 10 mL of distilled water and then sonicated for 30 min. The mixture was centrifuged at 10 000 rpm for 10 min. The supernatant was collected and mixed with cold ethanol 40% in a 1 : 1 (v/v) ratio at 4 °C in the freezer for 30 min and then centrifuged at 10 000 rpm for 30 min. The supernatant was collected and filtered with  $0.22 \mu\text{m}$  and the content of CNDs was measured using fluorescence spectroscopy at the excitation wavelength of 360 nm. Our results, depicted in Table 1, revealed that no CNDs were detected in the dough, while the highest concentration of CNDs was detected on the bread crust with  $512 \pm 1 \text{ mg kg}^{-1}$  DW. The difference in concentration of CNDs in breadmaking is supposed to be related to the temperature and heat treatment time, where the bread crust directly coming in contact with high temperature showed higher CNDs content than the bread crumb with  $322 \pm 4 \text{ mg kg}^{-1}$  DW. The possible relationship between CNDs and heat treatment has been reported since 2012 when CNDs were found in bread and caramelized sugars for the first time.<sup>39</sup>

The data are expressed as the mean  $\pm$  standard deviation. Values within the same column with different letters (a–e) were significantly different ( $P < 0.05$ ).

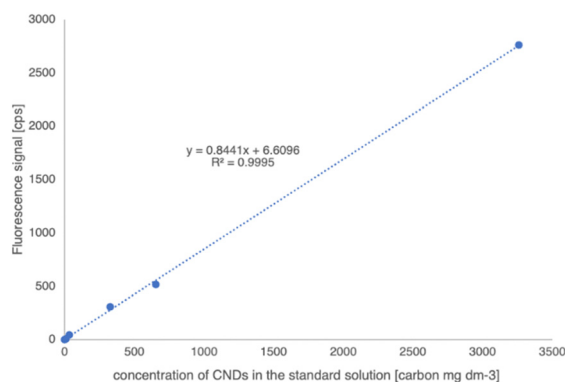


Fig. 7 A calibration curve with a purified M-CNDs standard solution measured using a Jasco FP-8500 spectrofluorometer. The carbon content of the standard was certified using a Primacs SNC 100 Carbon Nitrogen analyzer. Each concentration was measured in triplicate.



**Table 1** The concentration of CNDs in breadmaking

Food Items	Concentration of CNDs			
Dough		ND		
Bread crumb	322	±	4	mg kg <sup>-1</sup> in DW a
Bread crust	512	±	1	mg kg <sup>-1</sup> in DW b

This method's precision, repeatability, day-to-day variation, and linearity were assessed according to the validation procedure of the European Medicines Agency and AOAC International.<sup>40,41</sup> The standard curve was built with the regression line:  $y = 0,8441x + 6.61$  with  $R^2 = 0.9995$  with a limit of detection (LOD) of  $0.14 \text{ mg dm}^{-3}$  and a limit of quantification (LOQ) of  $0.47 \text{ mg dm}^{-3}$ . Considering the ten times dilution in the sample preparation, the detection limit calculated for the solid food sample is  $1.4 \text{ mg kg}^{-1}$ . With all the assessments, this method was reliable for measuring CNDs in foods.

## Conclusion

In conclusion, this study has demonstrated that the use of the Maillard reaction at low temperatures ( $120 \text{ }^\circ\text{C}$ ) and long time (12 h) is a promising method for synthesizing carbon nanodots (CNDs) with high fluorescence intensity and small size ( $2.5 \pm 0.5 \text{ nm}$ ). This study systematically explored the optimization of the synthesis of CNDs through the Maillard reaction, including (1) selecting an appropriate amino acid, (2) choosing the effective glycine-to-sucrose ratio, and (3) examining the influence of extraction solvents. Glycine enhanced the reactivity in the Maillard reaction, resulting in superior fluorescence intensity of CNDs compared to other amino acids. Moreover, the investigation into the glycine-to-sucrose ratio revealed that a 1 mmol:1 mmol ratio delivered the highest fluorescence intensity, offering a critical parameter for the synthesis of tailored CNDs. Expanding our exploration to extraction solvents, the crucial role of pH and ethanol concentration provided a valuable guide for controlling the fluorescence properties of CNDs, where 40% ethanol solution showed the most effective extraction to form CNDs with intense fluorescent intensity. The subsequent purification and characterization of Maillard reaction-derived carbon nanodots (M-CNDs) underscored the effectiveness of our isolation procedure. TEM imaging confirmed the nanosized, dark spherical morphology of M-CNDs, with an average size of  $2.5 \pm 0.5 \text{ nm}$ . The UV-Vis spectrum and intense blue fluorescence of M-CNDs further validated their exceptional properties. Raman spectroscopy analysis supported the absence of significant carbonaceous impurities, confirming the moderate graphitic structure of M-CNDs. The obtained M-CNDs were used as a standard for quantifying the CNDs' content in the breadmaking processing, where CNDs were only found in the bread crusts and crumbs after baking. It was shown that the presence of CNDs was closely related to the heat treatment process. The successful isolation and characterization of M-CNDs elevate the potential of these nanostructures in diverse applications, emphasizing

their role as a promising carbon dot source. The results of this study have the potential to advance the development of carbon nanodots for bioimaging, sensing, and other applications.

## Author contributions

Conceptualization, J. P. and D. H. H. N.; methodology, D. H. H. N.; doing experiments, D. H. H. N., A. M., J. P., L. N., and L. D.; analyzing data, D. H. H. N, A. M, and J. P.; writing – original draft preparation, A. M., D. H. H. N., L. N; writing – discussion and conclusion, H. E.-R., D. H. H. N., visualization, D. H. H. N., supervision, J. P., H. E.-R. All authors have read and agreed to the published version of the manuscript.

## Conflicts of interest

There are no conflicts to declare.

## Acknowledgements

The authors are thankful for the support of the Stipendium Hungaricum Scholarship Program and the grant No. K-132685 from National Research, Development and Innovation Office, Hungary.

## References

- X. Xu, R. Ray, Y. Gu, H. J. Ploehn, L. Gearheart, K. Raker and W. A. Scrivens, *J. Am. Chem. Soc.*, 2004, **126**, 12736–12737.
- H. Li, Z. Kang, Y. Liu and S.-T. Lee, *J. Mater. Chem.*, 2012, **22**, 24230.
- S. C. Ray, A. Saha, N. R. Jana and R. Sarkar, *J. Phys. Chem. C*, 2009, **113**, 18546–18551.
- S. Khan, A. Dunphy, M. S. Anike, S. Belperain, K. Patel, N. H. Chiu and Z. Jia, *Int. J. Mol. Sci.*, 2021, **22**, 6786.
- W. Zhang, H. Zhong, P. Zhao, A. Shen, H. Li and X. Liu, *Food Control*, 2022, **133**, 108591.
- D. Dhamodharan, H.-S. Byun, M. V. Shree, D. Veeman, L. Natrayan and B. Stalin, *J. Ind. Eng. Chem.*, 2022, **110**, 68–83.
- M. Pajewska-Szmyt, B. Buszewski and R. Gadzała-Kopciuch, *Spectrochim. Acta, Part A*, 2020, **236**, 118320.
- S. C. Pandey, A. Kumar and S. K. Sahu, *J. Photochem. Photobiol., A*, 2020, **400**, 112620.
- C. Cao and W. Guo, *Food Chem.*, 2024, **435**, 137578.
- F. Y. Vadia, S. Ghosh, V. N. Mehta, S. Jha, N. I. Malek, T. J. Park and S. K. Kailasa, *Food Chem.*, 2023, **428**, 136796.
- B. J. Wang, Z. Y. Xu, Z. Sun, Z. Q. Li, Y. H. Luo, H. Q. Luo and N. B. Li, *Anal. Bioanal. Chem.*, 2023, **415**, 4639–4647.
- M. A. Albalawi, H. Gomaa, M. A. El Hamd, M. A. S. Abourehab and M. A. Abdel-Lateef, *Luminescence*, 2023, **38**, 92–98.
- S. K. Tammina and J.-W. Rhim, *Chemosphere*, 2023, **313**, 137627.



- 14 A. Khan, Z. Riahi, J. Tae Kim and J.-W. Rhim, *Food Chem.*, 2024, **432**, 137215.
- 15 S. Chen, Q. Zeng, X. Tan, M. Ye, Y. Zhang, L. Zou, S. Liu, Y. Yang, A. Liu, L. He and K. Hu, *Carbohydr. Polym.*, 2023, **314**, 120938.
- 16 X. Gao, H. Zhang, L. Liu, M. Jia, X. Li and J. Li, *Food Chem.*, 2024, **432**, 137144.
- 17 D. Zhao, Z. Zhang, X. Liu, R. Zhang and X. Xiao, *Mater. Sci. Eng., C*, 2021, **119**, 111468.
- 18 K. Wang, Z. Gao, G. Gao, Y. Wo, Y. Wang, G. Shen and D. Cui, *Nanoscale Res. Lett.*, 2013, **8**, 122.
- 19 J. A. Jaleel and K. Pramod, *J. Controlled Release*, 2018, **269**, 302–321.
- 20 M. Tuerhong, Y. Xu and X.-B. Yin, *Chin. J. Anal. Chem.*, 2017, **45**, 139–150.
- 21 Z. Ji, Z. Yin, Z. Jia and J. Wei, *Langmuir*, 2020, **36**, 8632–8640.
- 22 E. Durantie, H. Barosova, B. Drasler, L. Rodriguez-Lorenzo, D. A. Urban, D. Vanhecke, D. Septiadi, L. Hirschi-Ackermann, A. Petri-Fink and B. Rothen-Rutishauser, *Biointerphases*, 2018, **13**, 06D404.
- 23 K. Hola, Y. Zhang, Y. Wang, E. P. Giannelis, R. Zboril and A. L. Rogach, *Nano Today*, 2014, **9**, 590–603.
- 24 S. Sahu, B. Behera, T. K. Maiti and S. Mohapatra, *Chem. Commun.*, 2012, **48**, 8835.
- 25 D. Li, X. Na, H. Wang, Y. Xie, S. Cong, Y. Song, X. Xu, B.-W. Zhu and M. Tan, *J. Agric. Food Chem.*, 2018, **66**, 1569–1575.
- 26 M. Saltmarch and T. P. Labuza, *Diabetes*, 1982, **31**, 29–36.
- 27 D. Li, Y. Xie, X. Na, Y. Li, C. Dai, Y. Li and M. Tan, *Food Funct.*, 2019, **10**, 4414–4422.
- 28 S. Matiacevich and M. Pilarbuera, *Food Chem.*, 2006, **95**, 423–430.
- 29 A. C. Ferrari and J. Robertson, *Philos. Trans. R. Soc. London, Ser. A*, 2004, **362**, 2477–2512.
- 30 Y.-M. Long, C.-H. Zhou, Z.-L. Zhang, Z.-Q. Tian, L. Bao, Y. Lin and D.-W. Pang, *J. Mater. Chem.*, 2012, **22**, 5917.
- 31 D. Li, X. Na, H. Wang, Y. Xie, S. Cong, Y. Song, X. Xu, B.-W. Zhu and M. Tan, *J. Agric. Food Chem.*, 2018, **66**, 1569–1575.
- 32 Y. Chen, H. Lin, Y. Li, M. Lin and J. Chen, *Ind. Crops Prod.*, 2019, **135**, 146–152.
- 33 J. B. Alexander Ross, W. R. Laws, K. W. Rousslang and H. R. Wyssbrod, in *Topics in Fluorescence Spectroscopy*, ed. J. R. Lakowicz, Kluwer Academic Publishers, Boston, 2002, vol. 3, pp. 1–64.
- 34 R. D'Souza and J. Powell-Tuck, *J. R. Soc. Med.*, 2004, **97**, 425–427.
- 35 J. Bai, Y. Ma, G. Yuan, X. Chen, J. Mei, L. Zhang and L. Ren, *J. Mater. Chem. C*, 2019, **7**, 9709–9718.
- 36 S. C. Shen and J. S. B. Wu, *J. Food Sci.*, 2004, **69**, FCT273–FCT279.
- 37 H. Ding, S.-B. Yu, J.-S. Wei and H.-M. Xiong, *ACS Nano*, 2016, **10**, 484–491.
- 38 R. Atchudan, T. N. J. I. Edison and Y. R. Lee, *J. Colloid Interface Sci.*, 2016, **482**, 8–18.
- 39 M. P. Sk, A. Jaiswal, A. Paul, S. S. Ghosh and A. Chattopadhyay, *Sci. Rep.*, 2012, **2**, 383.
- 40 I. ICH, *Topic Q 2 (R1) Validation of Analytical Procedures: Text and Methodology*. European Medicines Agency, CPMP/ICH/381/95, 1995.
- 41 AOAC International, 2016.

